

Surface spin-glass behavior in $\text{La}_{2/3}\text{Sr}_{1/3}\text{MnO}_3$ nanoparticles

T. Zhu,^{a)} B. G. Shen, J. R. Sun, H. W. Zhao, and W. S. Zhan

State Key Laboratory for Magnetism, Institute of Physics and Center for Condensed Matter Physics, Chinese Academy of Sciences, Beijing 100080, People's Republic of China

(Received 9 November 2000; accepted for publication 24 April 2001)

The low-temperature magnetic and transport properties of $\text{La}_{2/3}\text{Sr}_{1/3}\text{MnO}_3$ nanoparticles have been investigated. It is found that a surface spin-glass behavior exists in $\text{La}_{2/3}\text{Sr}_{1/3}\text{MnO}_3$ nanoparticles, which undergo a magnetic transition to a frozen state below 45 K. The low-temperature surface spin-glass behavior exists even at the highest field used ($H = 50$ kOe). Moreover, the spin-glass-like transition disappears for particles above 50 nm. In addition, the suppressed low-field magnetoconductivity (LFMC) observed at low temperature for nanosized $\text{La}_{2/3}\text{Sr}_{1/3}\text{MnO}_3$ is obviously lower than the expected upper limit of LFMC, 1/3, for polycrystalline manganites, which is proposed to arise from the higher-order tunneling through the insulating spin-glass-like surface layers. © 2001 American Institute of Physics. [DOI: 10.1063/1.1379597]

Magnetic nanoparticles have been a subject of intense research in the past decade because their unique magnetic properties make them very appealing from both the theoretical and technological points of view.^{1–4} One of the most controversial issues is the study of surface spin disorder or spin-glass behavior in the magnetic nanosized oxides. Some recent examples can be found in ball-milled CoFe_2O_4 (Ref. 2), NiFe_2O_4 (Ref. 3), and chemically precipitated $\gamma\text{-Fe}_2\text{O}_3$ (Ref. 4).

In the present work, we have studied the low-temperature magnetic and transport properties of doped manganite, $\text{La}_{2/3}\text{Sr}_{1/3}\text{MnO}_3$ nanoparticles, in particular the surface spin-glass behavior of the particles. The half-metallic perovskite manganites, such as $\text{La}_{2/3}\text{Sr}_{1/3}\text{MnO}_3$, are of great interest due to their colossal magnetoresistance effect. Recently, a good deal of progress to improve the low-field magnetoresistance (MR) response has been made for the polycrystalline samples,^{5–9} indicative of the promising candidates for the application in magnetoresistive devices. As a consequence, many investigations of the grain size effect on the magnetotransport or magnetic properties for manganites have also been presented. For example, an improved temperature dependence of MR has been presented in the nanosized $\text{La}_{2/3}\text{Sr}_{1/3}\text{MnO}_3$ formed by sol-gel processing.¹⁰ The high-field MR studies on ceramic $\text{La}_{2/3}\text{Sr}_{1/3}\text{MnO}_3$ as a function of the grain size suggest a noncollinear surface layer in granular $\text{La}_{2/3}\text{Sr}_{1/3}\text{MnO}_3$.¹¹ In our previous letter, we have reported the superparamagnetic behavior of the $\text{La}_{2/3}\text{Ca}_{1/3}\text{MnO}_3$ nanoparticles synthesized by mechanical milling.¹² But until now, the magnetic properties of nanosized manganites have not been exhaustively reported. In this letter, a surface spin-glass behavior of the nanosized $\text{La}_{2/3}\text{Sr}_{1/3}\text{MnO}_3$ has been carefully investigated. Moreover, the magnetotransport of the samples is also discussed on the basis of such novel magnetic properties.

The $\text{La}_{2/3}\text{Sr}_{1/3}\text{MnO}_3$ samples were prepared by a citric-gel process.¹³ The grain sizes of samples were directly ob-

tained by scanning electron micrograph. The average grain size D of granular $\text{La}_{2/3}\text{Sr}_{1/3}\text{MnO}_3$ is about 25 nm to 1.5 μm when sintered at 600 to 1300 °C, respectively. Magnetic properties of the samples have been measured using a commercial superconducting quantum interference device in the temperature range from 5 to 400 K and in applied magnetic fields up to 50 kOe. Magnetotransport have been measured using a standard four-probe dc method.

Figure 1 shows the temperature dependence of magnetization in the zero-field-cooled (ZFC) and field-cooled (FC) processes with an applied low field of 500 Oe for the nanosized $\text{La}_{2/3}\text{Sr}_{1/3}\text{MnO}_3$ (with mean sizes around 25 nm). Similar to our previous results for nanosized $\text{La}_{2/3}\text{Ca}_{1/3}\text{MnO}_3$ (Ref. 12), it can be seen that the ZFC curve exhibits a typical blocking process for the superparamagnetic particles with the blocking temperature at $T_B \approx 75$ K. A more important feature is that the FC curve reveals the existence of a sudden increase in magnetization below $T_F \approx 45$ K related, as we will see later, with the onset of the freezing process of the surface spin-glass layer for the nanosized $\text{La}_{2/3}\text{Sr}_{1/3}\text{MnO}_3$. This characteristic is much clearer in a careful measurement of the FC branch (inset of Fig. 1). A similar feature can also be seen in $\gamma\text{-Fe}_2\text{O}_3$ nanoparticles⁴ and such spin-glass-like behavior is

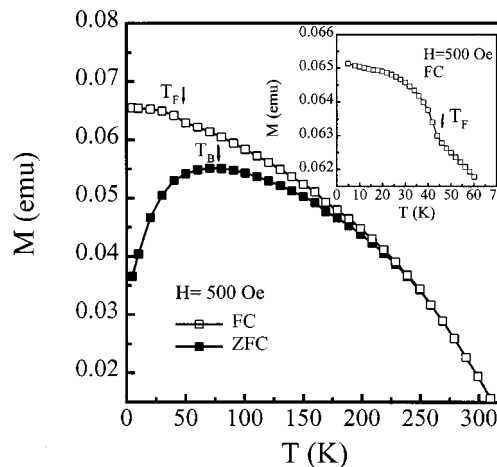


FIG. 1. Temperature dependence of low-field ZFC-FC magnetization of the nanosized $\text{La}_{2/3}\text{Sr}_{1/3}\text{MnO}_3$ ($D = 25$ nm) is shown. Inset: Detail of the FC branch showing the sudden decrease of the magnetization at about 45 K.

^{a)} Author to whom all correspondence should be addressed; Present address: Department of Physics and Astronomy, University of Delaware, Newark, Delaware, 19716; Electronic mail: zhutao@physics.udel.edu

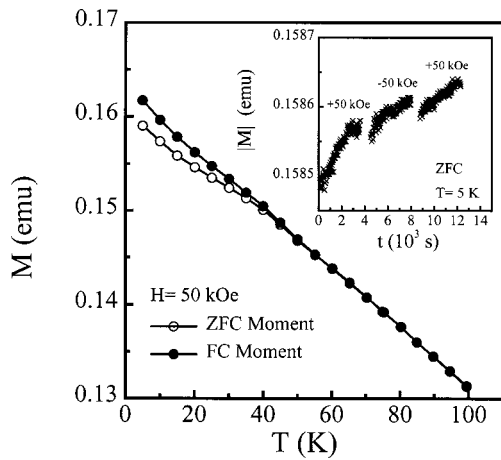


FIG. 2. High-field ZFC-FC processes showing the high field irreversibility in nanosized $\text{La}_{2/3}\text{Sr}_{1/3}\text{MnO}_3$ ($D=25$ nm) are shown. Inset: Time dependence of the absolute value of the magnetization in applied fields of alternated sign after a ZFC process.

denoted as a surface effect. This is to say the moments in the surface layer can freeze below T_F and align with the direction of moments in the core under a FC process. Thus, the magnetization exhibits a sudden increase below T_F .

Figure 2 shows that the irreversibility in magnetization remains below 45 K up to the highest field used ($H=50$ kOe) in ZFC-FC processes. This feature supports the existence of the surface spin-glass behavior in the $\text{La}_{2/3}\text{Sr}_{1/3}\text{MnO}_3$ nanoparticles because the field is very high (up to 50 kOe in our experiment) when compared with those typically used in the spin-glass bulks (few tens of Oe). Further support of the existence of the surface spin-glass behavior in the nanosized $\text{La}_{2/3}\text{Sr}_{1/3}\text{MnO}_3$ comes from the high-field relaxation processes in alternating fields after a ZFC process. The measurements were made by first cooling in zero field, then ramping the applied field to +50 kOe and then measuring every 30 s for 3600 s, ramping the field to -50 kOe, and measuring again for 3600 s. Finally, the field was ramped back to +50 kOe and measured again for 3600 s.^{3,4} The inset of Fig. 2 shows moment versus total elapsed time during this procedure. Absolute values of the moment are plotted on an expanded scale in order to compare +50 kOe and -50 kOe curves. Notice that an upward creep in the moment and subsequent iterations with positive and negative fields also result in continually higher values of magnetization, suggesting a structure of a ferromagnetic (FM) core that changes its orientation by coherent rotation plus a surface spin-glass layer that slowly relaxes in the direction of the field.

Figure 3 shows the grain size dependence of low-field FC magnetization for $\text{La}_{2/3}\text{Sr}_{1/3}\text{MnO}_3$, indicating that the spin-glass-like transition disappears with the increase of grain size. The high-field irreversibility is also strongly dependent on the particle size and has completely disappeared for the particles above 50 nm (when sintered above 800 °C as seen from the inset of Fig. 3). In other words, the surface layer is thinner with the increase in grain size, and then the surface effect also can not be measured. It is also worth mentioning that the critical size of disappearance of surface spin-glass behavior for $\text{La}_{2/3}\text{Sr}_{1/3}\text{MnO}_3$ grains is larger than for other nanosized magnetic oxides.^{3,4} Moreover, the sur-

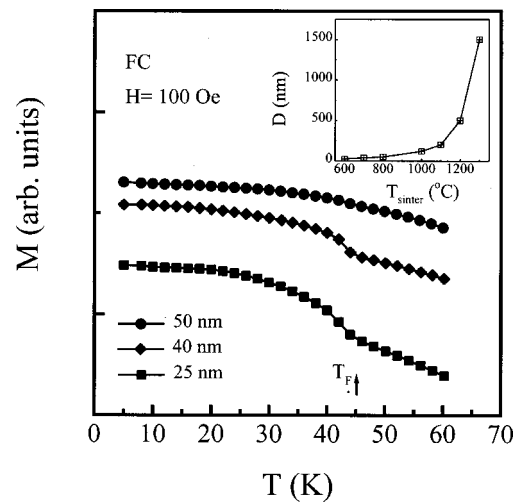


FIG. 3. The size dependence of low-field FC M - T curves for $\text{La}_{2/3}\text{Sr}_{1/3}\text{MnO}_3$ is shown. Inset: The average grain size D of granular $\text{La}_{2/3}\text{Sr}_{1/3}\text{MnO}_3$ when sintered from 600 to 1300 °C.

face spin-glass behavior in $\text{La}_{2/3}\text{Sr}_{1/3}\text{MnO}_3$ nanoparticles can be independent of the actual Mn^{4+} contents in our samples because it only changes minimally for the Mn^{4+} content in the samples annealing from 600 to 800 °C.

Considering that the Mn^{3+} - Mn^{4+} double-exchange mechanism is mainly responsible for the magnetism and conduction of the doped manganite $\text{La}_{2/3}\text{Sr}_{1/3}\text{MnO}_3$, the origin of the surface spin-glass layers formation in the $\text{La}_{2/3}\text{Sr}_{1/3}\text{MnO}_3$ nanoparticles may be due to the existence of broken bonds at the surface and the translational symmetry breaking of the lattice, generating randomness in the double-exchange interactions. Hence, the Mn environment at the surface is not the same as that inside the grains, inducing disordered spins at the grain surface. In other words, a core-shell type structure can be proposed: the core is metallic and FM and the shell is insulating and spin disordering. Although it is difficult to directly assert that disorder is confined in a well delimited surface layer or a progressive disorder process from the inner part of the particles to the surface, the core-shell structure model is suitable for the $\text{La}_{2/3}\text{Sr}_{1/3}\text{MnO}_3$ nanoparticles and consistent with the results of temperature dependence of FC magnetization (Fig. 1) and relaxation process of magnetization in altering fields (Fig. 2). Moreover, the numerical calculation in Ref. 3 also suggests such a core-shell structure in the nanomagnetic oxides. The existence of a distorted structure at the surface of the manganite nanoparticles has also been indirectly supported by the observation of a surface phonon,¹⁴ which was seen from the IR spectra for $\text{La}_{2/3}\text{Ca}_{1/3}\text{MnO}_3$ samples with small grain size.

To assess the nature of resistivity and relevant intergrain tunneling MR, we measured the temperature and magnetic field dependence of resistivity for $\text{La}_{2/3}\text{Sr}_{1/3}\text{MnO}_3$ with different grain sizes. Figure 4 shows the temperature dependence of the normalized zero field resistivity $R(T)/R(300\text{ K})$ for $\text{La}_{2/3}\text{Sr}_{1/3}\text{MnO}_3$ with varying grain size D . The upturn observed in the low-temperature resistance for nanosized $\text{La}_{2/3}\text{Sr}_{1/3}\text{MnO}_3$ indicates an insulating-like barrier in the nanosized $\text{La}_{2/3}\text{Sr}_{1/3}\text{MnO}_3$, due to the damage of the double-exchange mechanism in the disordered interfacial region. Moreover, the insulating-like barrier of our samples becomes

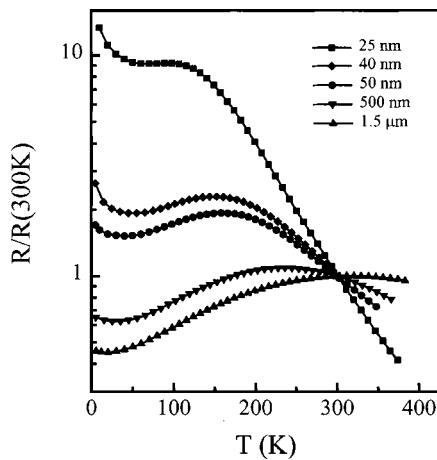


FIG. 4. The temperature dependence of the normalized zero field resistivity $R(T)/R(300\text{K})$ for granular $\text{La}_{2/3}\text{Sr}_{1/3}\text{MnO}_3$ with varying grain size D is shown.

higher with a decrease in grain sizes and the details will be published elsewhere.

Figure 5 shows the magnetic field dependence of the conductivity $\sigma(H)$ at 5 K for $\text{La}_{2/3}\text{Sr}_{1/3}\text{MnO}_3$ with varying grain size D , normalized by the zero field value σ_0 . For all samples, $\sigma(H)$ is quite linear with an applied field in the high field region ($H > 0.5\text{ T}$), and the slope of the field dependence increases monotonically with the decrease of D . Furthermore, our results indicate that the general characteristic of linear dependence of $\sigma(H)$ with an applied field in the high-field region appears to be independent of not only Curie temperature, T_C (Ref. 15), but also grain size D , for polycrystalline manganites. The inset of Fig. 5 shows the grain size dependence of the low-field magnetoconductivity (LFMC) at 5 K for $\text{La}_{2/3}\text{Sr}_{1/3}\text{MnO}_3$, which is defined by the extrapolation towards zero field of the initial drop of the high-field dependence of the conductivity $\sigma(H)/\sigma_0$. It is clear that the LFMC of 25 nm $\text{La}_{2/3}\text{Sr}_{1/3}\text{MnO}_3$ is 0.187, which is obviously lower than the general upper limit value of 1/3, for polycrystalline manganites.¹⁵ Similar results can be seen in the milled nanosized $\text{La}_{2/3}\text{Sr}_{1/3}\text{MnO}_3$.¹¹ Also from the high-field MR in milled samples, a noncollinear surface layer was proposed. However, our magnetic results give di-

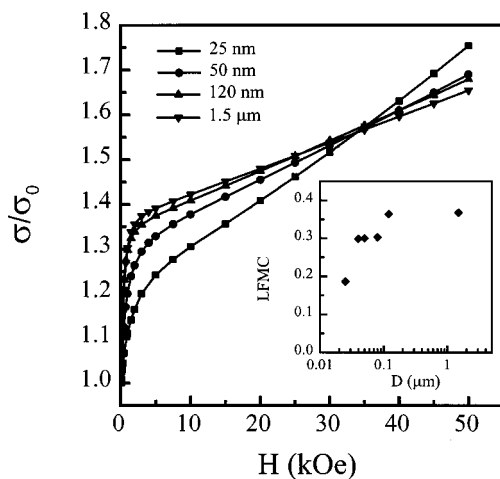


FIG. 5. The magnetic field dependence of the normalized conductivity at 5 K for $\text{La}_{2/3}\text{Sr}_{1/3}\text{MnO}_3$ with varying grain size is shown. Inset: The grain size dependence of LFMC.

rect evidence for the existence of spin-glass or spin disorder layers at the surface of nanosized manganites.

Very different from classical tunneling mechanisms in FM metal-insulator systems,¹⁶ the intergrain conductivity is dominated by a second-order tunneling process,¹⁵ where the e_g electron tunnels through surfacial spin sites at the grain boundary in the polycrystalline manganites and the spin of the hopping electron is aligned with the local t_{2g} moment during the conduction process. The upper limit for the conductivity rise just after saturation is 1/3, which is independent of T_C . Notice that such second-order tunneling is the simplest spin-flip process arising from a single interfacial spin site. In other words, the second-order tunneling should only be available for the narrow interface boundary in the μm -sized manganites where the thickness of the grain boundary with structural disorder is estimated to be of the order of 1 nm.⁶ However, the temperature dependence of resistance indicates that the insulating-like barriers become higher with decreasing of grain size (Fig. 4), thus, the thickness of the grain boundary is also enlarged. Hence higher-order tunneling should be considered when the second-order tunneling process of e_g electron, from grain 1 to the boundary state then grain 2, are broken in the case of the enlarged grain boundary for the nanosized samples. This is to say that the extra inelastic tunneling may dominant and the LFMC is suppressed considering that extra spin-flip effect arises from the disordered spin sites in the spin-glass-like insulating surface layers in nanosized $\text{La}_{2/3}\text{Sr}_{1/3}\text{MnO}_3$. When the surface spin-glass behavior disappears with the increase of grain size or decrease of thickness of the grain boundary (as shown in Fig. 3), the second-order tunneling should dominant and the LFMC increases to about 1/3.

This project was supported by NSFC and the State Key Project of Fundamental Research of MOST (G1998061300).

¹ *Magnetic Properties of Fine Particles*, edited by J. L. Dorman and D. Fiorani (North-Holland, Amsterdam, 1992).

² D. Lin, A. C. Nunes, C. F. Majkrzak, and A. E. Berkowitz, *J. Magn. Magn. Mater.* **145**, 343 (1995).

³ R. H. Kodama, A. E. Berkowitz, E. J. McNiff, Jr., and S. Foner, *Phys. Rev. Lett.* **77**, 394 (1996).

⁴ B. Martínez, X. Obradors, L. I. Balcells, A. Rouanet, and C. Monty, *Phys. Rev. Lett.* **80**, 181 (1998).

⁵ H. Y. Hwang, S. W. Cheong, N. P. Ong, and B. Batlogg, *Phys. Rev. Lett.* **77**, 2041 (1996).

⁶ A. Gupta, G. Q. Gong, G. Xiao, P. R. Duncombe, P. Lecoeur, P. Trouiloud, Y. Y. Wang, V. P. Dravid, and J. Z. Sun, *Phys. Rev. B* **54**, 15629 (1996).

⁷ R. Shreekala, M. Rajeswari, K. Ghosh, A. Goyal, J. Y. Gu, C. Kwon, Z. Trajanovic, T. Boettcher, R. L. Greene, R. Ramesh, and T. Venkatesan, *Appl. Phys. Lett.* **71**, 282 (1997).

⁸ J. M. D. Coey, *J. Appl. Phys.* **85**, 5576 (1999).

⁹ X. L. Wang, S. X. Dou, H. K. Liu, M. Ionescu, and B. Zeimetz, *Appl. Phys. Lett.* **73**, 396 (1998).

¹⁰ R. Mahesh, R. Mahendiran, A. K. Raychaudhuri, and C. N. R. Rao, *Appl. Phys. Lett.* **68**, 2291 (1996).

¹¹ L. Balcells, J. Fontcuberta, B. Martínez, and X. Obradors, *Phys. Rev. B* **58**, R14697 (1998).

¹² R. W. Li, H. Xiong, J. R. Sun, Q. A. Li, Z. H. Wang, J. Zhang, and B. G. Shen, *J. Phys.: Condens. Matter* **13**, 141 (2001).

¹³ T. Zhu, C. H. Yan, Z. M. Wang, H. W. Zhao, J. R. Sun, and B. G. Shen, *Solid State Commun.* **117**, 471 (2001).

¹⁴ L. Zheng, K. B. Li, and Y. H. Zhang, *Phys. Rev. B* **58**, 8613 (1998).

¹⁵ S. Lee, H. Y. Hwang, B. I. Shraiman, W. D. Ratcliff, and S. W. Cheong, *Phys. Rev. Lett.* **82**, 4508 (1999).

¹⁶ T. Zhu and Y. J. Wang, *Phys. Rev. B* **60**, 11918 (1999).